Ultraviolet Laser Development for Planetary Lander Missions

Molly Fahey, Anthony Yu, Andrej Grubisic, Stephanie Getty
NASA Goddard Space Flight Center
8800 Greenbelt Rd, Greenbelt, MD 20771
Molly.e.fahey@nasa.gov, Anthony.w.yu@nasa.gov, Andrej.grubisic@nasa.gov, Stephanie.a.getty@nasa.gov

Ricardo Arevalo Jr.
Department of Geology
University of MD, College Park, MD 20742
rarevalo@umd.edu

Xiang Li
Center for Space Science and Technology
University of MD Baltimore County, Baltimore, MD 21250
Xiang.li@nasa.gov

Richard Liu
Department of Electrical and Computer Engineering
University of IL at Urbana-Champaign, Urbana, IL 61801
Rliu37@illinois.edu

William Mamakos
Design Interface, Inc.
3451 Gamber Road, Finksburg, Maryland 21048
william.mamakos@designinterfaceinc.com

Abstract—**Mass spectrometers represent progressive analytical platforms for future *in situ* lander missions to explore the surface chemistry of planetary bodies. Europa (as an astrobiology objective) and the Moon (an extension of the terrestrial system) are two primary targets for future NASA missions to search for extraterrestrial life and potentially habitable environments beyond Earth, further our understanding of the timing and formation of the Solar System, and identify potentially viable economic resources such as water and/or valuable metal assets. The CORALS (Characterization of Ocean Residues And Life Signatures) and CRATER (Characterization of Regolith And Trace Economic Resources) instruments are laser-based Orbitrap™ mass spectrometers currently under development for prospective lander missions to Europa and the Moon, respectively. We report on the advancement of two compact, robust, and high technology readiness level (TRL) ultraviolet (UV) solid state lasers that serve as the sampling and ionization sources of these two investigations.**

Table of Contents

978-1-7821-2734-7/20/$31.00 ©2020 IEEE

1. Introduction

The CORALS (Characterization of Ocean Residues And Life Signatures) and CRATER (Characterization of Regolith And Trace Economic Resources) investigations center on two distinct laser-enabled Orbitrap™ mass spectrometers that are being developed currently through the NASA ROSES Instrument Concepts for Europa Exploration (ICEE 2) and Development and Advancement of Lunar Instrumentation (DALI) programs, respectively. The CORALS/ICEE 2 project is a two year technology maturation effort targeting the build and demonstration of an instrument adapted for the detection and unambiguous identification of biosignatures embedded in icy samples for a prospective Europa lander mission. In comparison, the CRATER/DALI project is a three year endeavor to advance to TRL 6 (system-level validation in a relevant environment) an instrument capable of mapping mineralogy and major/minor element abundances in lunar surface materials for a future lander opportunity.

One of the major differences between the CORALS and CRATER instrument designs is the laser sources required to meet the science objectives of these investigations (outlined below). The CORALS laser generates >450 µJ/pulse energy at 266 nm, a wavelength that maps to the Mars Organic Molecule Analyzer (MOMA) instrument onboard the ExoMars rover, whereas the CRATER laser generates >1 mJ/pulse energy at 213 nm, a deeper UV wavelength to augment photon-substrate coupling with geological phases found on the lunar surface. Both lasers operate between 1-10 Hz pulse repetition frequency (PRF) with a 5 ns pulse duration, variable energy attenuation between 1-100%, and controlled beam steering to raster across the sample surface and provide 2D chemical imaging. The CORALS laser is a side-pumped Cr:Nd:YAG laser oscillator with a fundamental wavelength of 1064 nm and fourth harmonic generator to achieve an output wavelength of 266 nm. The CRATER laser is a side-pumped Cr:Nd:YAG master oscillator power amplifier (MOPA) laser with a fundamental wavelength of 1064 nm and fifth harmonic generator to achieve an output wavelength of 213 nm. Both lasers derive from heritage systems, and each has been designed to minimize the Size, Weight, and Power (SWaP) requirements for potential lander applications. Here, we discuss the design, trade studies, prototype performance, preliminary test and analysis results of the CORALS and CRATER ultraviolet lasers.

2. Science Objectives

Europa (an astrobiology objective) and the Moon (an extension of the terrestrial system) are primary targets for near-term NASA and international mission concepts. Europa represents a potentially viable world, and may host an extant ecosystem in the subsurface ocean that could transmit chemical signals to the surface via mass exchange facilitated by ocean dynamics and ice tectonics. The lunar (sub)surface provides a window into: chemical and isotopic fractionation provoked by the Moon-forming event; the influx and accumulation of prebiotic organic matter in the inner Solar System; the distribution of potentially viable economic resources, such as water and/or valuable metals; and, a reference point for calibrating the crater counting record.

Both of these targets, which are of strategic value to the science community, require highly capable instrumentation to characterize the composition of surface and near-surface materials *in situ*. Consequently, for the exploration of these planetary environments, NASA has invested in the development of two laser-enabled mass spectrometers: CORALS (for the analysis of ocean-derived salts and ice residues) and CRATER (for the analysis of regolith and rock). Both instruments rely on an Orbitrap™ mass analyzer that offers ultrahigh mass resolving powers up to $m/\Delta m > 10^6$ (FWHM at mass 100 Da; [1]) and sub-ppm mass accuracy [2], and can be integrated with a pulsed laser system for *in situ* chemical analysis [3]. Laser desorption/ablation mass spectrometry, as realized by these pioneering instruments, provides an ideal way to characterize precious sample specimens with high spatial resolution (limited only by the beam diameter and angle of incidence) and specificity (via controlled fluences), and without requiring contact with the sample (reducing cross-contamination risks). Laser-based sampling methods are particularly well suited for planetary exploration as they consume only ng of material per shot, versus traditional pyrolysis techniques that require upwards of tens of mg of sample per experiment, such as those conducted by Viking, Phoenix and the Mars Science Laboratory (MSL).

During laser microprocessing, both positive and negative ions are formed from the pulsed laser plasma. As opposed to near infrared (e.g., 1064 nm = 1.2 eV/ photon) and visible light (e.g., 532 nm = 2.3 eV/photon), the energies of photons generated at ultraviolet (UV) wavelengths (e.g., 266 nm = 4.7 eV/photon) approach the band gap energies of many planetary materials (≥ 4.0 eV; e.g., [4]). Further, only two UV photons are required to access the 1st ionization energies of nearly the entire periodic table (outside the halogens and noble gases; [5]) and most organic molecules, such as nucleotides [6], amino acids [7], and polycyclic aromatic hydrocarbons [8]. Consequently, many commercial laser desorption/ablation systems use Nd:YAG gain media (emission at 1064 nm) and a series of frequency multiplying nonlinear crystals to access ultraviolet wavelengths, such as 266 nm (fourth harmonic) or 213 nm (fifth harmonic). For geological applications, shorter wavelengths also enhance photon absorption by optically translucent/transparent substrates [9]. Whereas low radiant exposures (i.e., fluences < 1 J/cm^2) provide sufficient photon fluxes to ionize alkali metals and volatile organic compounds, higher fluences (i.e., >1 J/cm^2) are essential to analyze refractory organics and geological phases that require multiphoton ionization. Access to fluences in excess of the ablation threshold may also be exploited to induce molecular fragmentation and promote disproportionation reactions, enabling the derivation of molecular structure by in-source decay (ISD; [10]).

The first laser desorption/ablation mass spectrometer flown into space was carried on the Phobos-Grunt mission [11], but a thruster malfunction prevented the spacecraft from escaping low Earth orbit, resulting in an uncontrolled re-entry and crash into the Pacific Ocean. As such, the Mars Organic Molecule Analyzer (MOMA) instrument onboard the ExoMars rover (scheduled to launch in 2020) will establish the first laser-enabled mass spectrometer on another planet (assuming successful deployment) [12,13,14]. The prime objective of the MOMA investigation is to search for signs of past or present life on Mars through a detailed chemical analysis of the Martian surface. Although the instrument has the capacity to measure inorganic compounds, the main focus of MOMA is the detection and structural characterization of organic compounds that may be present and preserved in Martian near-subsurface samples over a range of molecular weight. The laser desorption mode on MOMA was specifically developed to enable detection and structural analysis of nonvolatile organic compounds up to 1 kDa [14,15].

The MOMA laser system, which represents a major step forward in optical engineering, centers on a passively Q-switched Nd:YAG oscillator coupled with a two-stage frequency quadrupling that produces 266 nm radiation in 1.5 ns pulses with an output energy of 130 μJ that can be attenuated via thermal tuning of the nonlinear crystals to less than 10% of the maximum energy output [14,16,17].

Recently, a 266 nm laser (albeit a commercial system) was interfaced directly (i.e., without an intermediary linear ion trap or C-Trap) to an Orbitrap™ mass analyzer that has been ruggedized for the rigors of spaceflight, thereby representing a proof-of-concept of the CORALS and CRATER instrument designs. This prototype system has been shown to: i) detect major elements (mineralogical indicators) and organic molecules (potential biosignatures) with ultrahigh mass resolution ($m/\Delta m \geq 10^5$, FWHM) and detection limits down to $pmol/mm^2$ levels; ii) quantify isotopic abundances with <1.0% (2σ) precision; and, iii) identify molecular stoichiometry via highly accurate mass measurements within 3 ppm of absolute values [18]. Thus, the next generation CORALS and CRATER instruments supported through the laser development effort described here represent potentially game-changing payload options for exploration of Europa, the Moon, and a host of other planetary targets.

3. UV LASER REQUIREMENTS

To support the efficient ablation of translucent minerals and amorphous phases, the CRATER investigation requires a high-power, solid-state laser that leverages the heritage master oscillator power amplifier (MOPA) flown on the Mercury Laser Altimeter (MLA) instrument but quintuples the frequency to produce ≥ 1 mJ of deep ultraviolet light (213 nm, equating to 5.8 eV/photon). The CORALS laser, on the other hand, more closely resembles the 266 nm (4.7 eV/photon) laser system flown on MOMA, though the CORALS design produces more than three times the maximum output energy and finer attenuation control.

The CORALS and CRATER lasers have different UV wavelengths and pulse energy requirements due to their specific science objectives, but other parameters and features are quite similar. Table 1 summarizes the two programs and requirements. Both lasers leverage the use of high TRL and proven laser designs for generating the fundamental wavelength at 1064 nm to convert to the necessary UV wavelengths and pulse energies. The following sections will describe in more detail the design and approach for each laser transmitter.

4. UV LASER DESIGN

The CORALS laser is a diode pumped, zig-zag Cr:Nd:YAG slab passively Q-switched oscillator similar to the Lunar Orbiter Laser Altimeter (LOLA) laser [19]. A similar oscillator design was used on the Mercury Laser Altimeter (MLA) [20], and the Geoscience Laser Altimeter System (GLAS) [21], where amplifier stages were used to generate higher pulse energy. The CORALS laser generates a fundamental 1064 nm wavelength, and with fourth harmonic generation (4HG) achieves an UV output of 266 nm. The CORALS laser is capable of generating ≥450 μJ/pulse at 266 nm. This corresponds to three times the pulse energy of the MOMA laser (130 μJ/pulse at 266 nm) [16]. The laser output is focused to a 50 μm diameter focal spot size (though this is a negotiable parameter that may be adjusted to meet mission goals), and may be actively scanned across a 500 μm diameter sample area with a MEMS steering mirror. The laser energy is variable between 1-100% to optimize the fluence at the sample. Two photodetectors are located in the laser enclosure for start pulse detection and triggering the instrument measurement sequence, and energy monitoring. A schematic of the CORALS laser is shown in Figure 1.

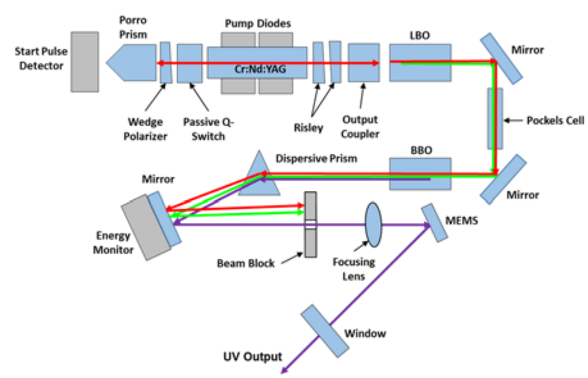

Figure 1. CORALS laser schematic (flight design).

Table 1. Laser requirements for the CORALS and CRATER instruments.

	CRATER	CORALS
Program	DALI	ICEE 2
Period of Performance	3 Years	2 Years
Targeted Mission	Moon	Europa
Laser Baseline	MLA Master Oscillator Power Amplifier	GLAS/LOLA/MLA Master Oscillator
Mission Lifetime	1 MShots	10 MShots
Output Wavelength	213 nm	266 nm
Frequency Conversion	5^{th} Harmonic of 1064 nm	4^{th} Harmonic of 1064 nm
DHMR / Radiation	Yes (115°C for 60 Hrs) / 20 krad	Yes (115°C for 60 Hrs) / 300 krad
UV Pulse Energy	>1 mJ	>450 μJ
Beam Spot Size (Diameter)	50 μm	50 μm
Peak Intensity	50 J/cm^2	20 J/cm^2
Pulse Rate	1-10 Hz	1-10 Hz
Beam Steering and Energy Attenuation	Beam Steering: YES, <±10º; Attenuation: 1 - 100% (in increment of 5% - objective, 1% - goal)	

The CORALS oscillator uses two, 200W, single bar (G1 package, Cutting Edge Optronics) laser diode arrays (LDA) with center wavelength of 808 nm at 27°C operating temperature to side-pump a Brewster cut, 26.8 mm long, trapezoidal laser slab. A Cr^{4+}:YAG with 0.46 optical density saturable absorber is used to generate laser pulses of approximately 5 ns (FWHM). The oscillator cavity uses a Porro prism high reflector to minimize the sensitivity to misalignment and a plano-mirror output coupler with 50% reflectivity at 1064 nm. Risley wedges are used to align the laser cavity and a wedge quartz rotator is used for both alignment and polarization control. The LDAs are heat sunk to an aluminum laser bench and maintained at a slightly elevated temperature of 27 ± 1°C to maintain active thermal control in a Europa lander vault susceptible to thermal drift over the range of -40°C to +25°C. The output beam of the CORALS fundamental laser is TEM_{00} with a ~ 800 μm full width at $1/e^2$ and an $M^2 \sim 1.2$.

The fundamental oscillator output wavelength is frequency quadrupled to achieve 266 nm using non-linear optical frequency conversion. A LBO (lithium triborate) crystal converts 1064 nm to 532 nm, and a BBO (beta barium borate) crystal converts 532 nm to 266 nm. Both the LBO (θ=90°, ϕ=9.9°) and BBO (θ=47.7°) crystals are designed for Type I critical phase matching at an operating temperature above the oscillator at 60°C to ensure active thermal control. Both LBO and BBO crystals are radiation insensitive and have showed negligible degradation after exposure to 200 krad total dose based on a study led by the German Space Agency [22]. LBO has flown on previous space laser instruments including GLAS and ATLAS [21,23]. Two LBO crystals with dimensions 3 x 3 x 10 mm^3 are arranged for spatial walk-off compensation with birefringence angles aligned 180° to each other to maximize the conversion efficiency and beam quality [24,25]. Four BBO crystals with dimensions 3 x 3 x 5 mm^3 are arranged with alternating birefringence angles aligned 180° to each other for optimum walk-off compensation [26].

The CORALS laser energy must be tunable between 1-100% with a resolution requirement of 5% (and a goal of 1%) to achieve the optimal pulse energy for science measurements. The active energy attenuation is enabled through the use of a Pockels cell located between the LBO and BBO crystals to control the incident 532 nm polarization orientation relative to the nonlinear crystal optical axis and vary the conversion efficiency to 266 nm. In order to achieve efficient second harmonic generation (SHG) the polarization of the input laser must be phase matched to the nonlinear optical crystal. By rotating the polarization of the 532 nm laser prior to the BBO crystal we change the phase matching condition and therefore vary the conversion to 266 nm. The output laser energy is attenuated as a function of the Pockels cell drive voltage between 0-800 V.

The 266 nm output is separated from the residual 1064 nm and 532 nm laser light with a CaF_2 dispersive prism, and focused to a spot size of 50 μm at the sample. A MEMS steering mirror (Mirrorcle Technologies, Inc) scans the output beam over a 500 μm diameter area, enabling raster patterns such as that shown in Figure 2.

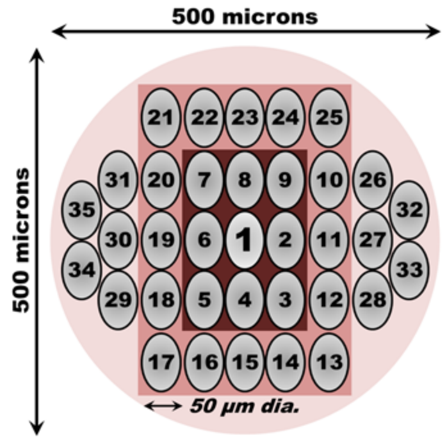

Figure 2. Raster scan pattern produced by MEMS steering mirror of the CORALS UV laser at the sample.

A start pulse detector is located behind the Porro prism to monitor the leakage from the oscillator and provide a trigger pulse to the instrument to initiate the timing sequence. The start pulse detector is a JQ5P quadrant Si-photodiode. An UV-enhanced SiC-photodiode (JQA5) is located after the dispersive prism to monitor the laser energy at 266 nm.

The opto-mechanical design for the CORALS laser is based on heritage and lessons learned from previously developed space-flight lasers at NASA Goddard Space Flight Center (GSFC) including GLAS, MLA, and LOLA. The laser enclosure and opto-mechanical mounts are made of aluminum. The laser slab mount, LDA mount, and nonlinear crystal mounts are all made of copper for improved thermal conductivity. The laser bench is maintained at a temperature of 27 ± 1°C with resistive heaters. The non-linear crystals are thermally isolated from the laser bench and maintained at an elevated temperature of 60 ± 1°C with resistive heaters. The CORALS mechanical model is shown in Figure 3. The overall dimensions are 18 x 8.1 x 3.6 cm^3. The total mass for the laser is 750 g. Due to the well-known risk of laser induced contamination damage with UV lasers in space, as well as the requirement for the laser to survive Dry Heat Microbial Reduction (DHMR, e.g. 115°C for 60 hours), the use of epoxies and other outgassing materials are limited in this design [27,28,29,30,31,32,33,34,35,36]. Additionally, the laser enclosure is back-filled with clean dry air (CDA) and pressurized to >1 atm. The CaF_2 output window is welded to a stainless steel flange using femtosecond laser welding. The stainless steel flange and lid are secured to the laser enclosure with mechanical fasteners and metal c-seals to create a hermetic seal.

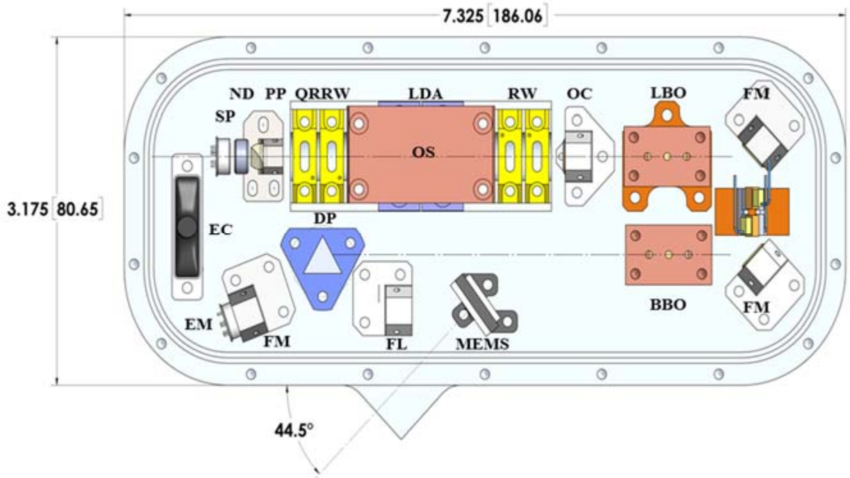

SP	Start Pulse Detector	LBO	Lithium Triborate
ND	Neutral Density Filter	BBO	Beta Barium Borate
PP	Porro Prism	FM	Fold Mirror
QR	Quartz Rotator	DP	Dispersive Prism
RW	Risley Wedge	EM	Energy Monitor
LDA	Laser Diode Arrays	FL	Focusing Lens
OS	Oscillator Slab	MEMS	Microelectromechanical System Mirror
OC	Output Coupler	EC	Electrical Connector

Figure 3. CORALS UV laser model.

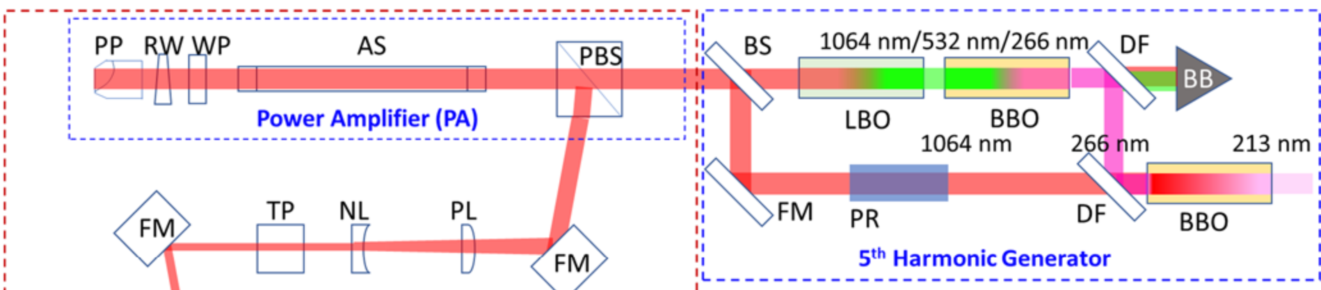

PP	Porro Prism	DF	Dichroic Filter
WP	Waveplate	FM	Fold Mirror
TP	Tilt Plate	BS	Beam Splitter
RW	Risley Wedge	PBS	Polarization Beam Splitter
BB	Beam Block	PQS	Passive Q-Switch
NL	Negative Lens	PL	Positive Lens
OS	Oscillator Slab	AS	Amplifier Slab
PR	Polarization Rotator		

Figure 4. CRATER UV laser design.

The CRATER laser is a high power Cr:Nd:YAG MOPA laser based on the MLA laser transmitter, and with fifth harmonic generation (5HG) achieves an output wavelength of 213 nm [20]. A schematic of the CRATER laser is shown in Figure 4.

The master oscillator (MO) is a crossed-Porro optical resonator with polarization output coupling, a Brewster cut, Cr:Nd:YAG slab pumped by a single two-bar stack (G2 package from Coherent, Inc.) of GaInAsP laser diode array (LDA), an air gap polarizer, a passive Q-switch saturable absorber (Cr^{4+}:YAG, 0.46 optical density), zero-order quartz wave plates for polarization control, and fused-silica Risley wedges for optical alignment. A thermoelectric cooler (TEC) is used to regulate the temperature of the LDA, which is heat sunk to the laser bench to keep the oscillator LDA at its design temperature and aligned to the absorption peak of the gain crystal. The 0.5% Cr^{3+} co-doping of the Cr:Nd:YAG slab enhances the resistance to radiation darkening. The nominal MO mode diameter is 1.0 mm, and its output energy is 3.0 mJ in a 5-ns pulse [20].

The MO output beam undergoes a beam expansion (2× magnification) and is amplified ~7× by double passing through a power amplifier (PA) stage. The Cr:Nd:YAG PA slab is pumped by two, four-bar stacks of GaInAs LDAs (2× G4 packages). The injected MO signal is double-passed through the PA to generate the required energy for the instrument. The isolation of the amplifier output beam from its input beam is accomplished by polarization. A 0.57-retardation wave plate together with the Porro-prism reflector provides a polarization change in the back-reflected beam to the orthogonal linear polarization. The PA amplifies the MO energy from ~3 mJ to a nominal laser pulse energy of ~20 mJ.

The 1064 nm output from the MOPA laser is converted to 213 nm using three non-linear optical crystals (1 × LBO and 2 × BBO) in series to generate the fifth harmonic. The 1064 nm is divided into two beam paths. The first beam path is used for the generation of the fourth harmonic at 266 nm using Type I LBO and BBO as in the CORALS laser described earlier. The second beam path of the 1064 nm is then mixed with the 266 nm in a Type I BBO crystal (θ=51.2°) to generate the fifth harmonic at 213 nm.

Energy attenuation is achieved by placing the Pockels cell in the second beam path of the 1064 nm. Analogous to the CORALS laser, the output energy can be adjusted by adjusting the input polarization state of the 1064 nm into the BBO crystal.

Also, similar to the CORALS design, the 213 nm output is separated from the residual 1064 nm, 532 nm, and 266 nm laser light with a dispersive prism, and focused to a 50 µm diameter spot size at the sample. A MEMS steering mirror (Mirrorcle Technologies, Inc) scans the output beam over a 500 µm diameter area raster pattern shown in Figure 2.

5. UV Laser Performance and Analysis

We built a breadboard CORALS laser to demonstrate the performance at 266 nm. The schematic of the breadboard laser is shown in Figure 5.

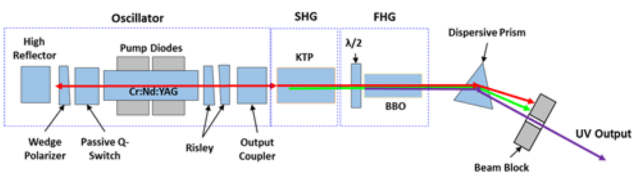

Figure 5. Schematic of CORALS breadboard laser currently in operation at NASA GSFC.

The breadboard oscillator is the same as the CORALS oscillator design described in Section 4 except a plano/plano mirror cavity configuration is used for ease of alignment and testing. A Type II KTP (potassium titanyl phosphate) crystal (θ=90.0°, ϕ=23.5°) operating at 27°C is used for SHG to 532 nm. A Type I BBO crystal operating at room (~25°C) is used to convert the 532 nm to 266 nm. A dispersive prism separates the 266 nm output from the residual 1064 nm and 532 nm light. The CORALS breadboard characterization results are summarized in Figure 6. The performance of the 266 nm laser was measured at a pulse repetition frequency of 20 Hz, pump pulse duration of 200 µs, and LDA current of 115 A. The switch-out time for the Q-switch pulse was approximately 180 µs from the beginning of the pump pulse. The measured pulse energy at 266 nm was 450 µJ corresponding to a fourth harmonic frequency conversion efficiency of 16%. The pulse width at 266 nm was measured to be 5.2 ns.

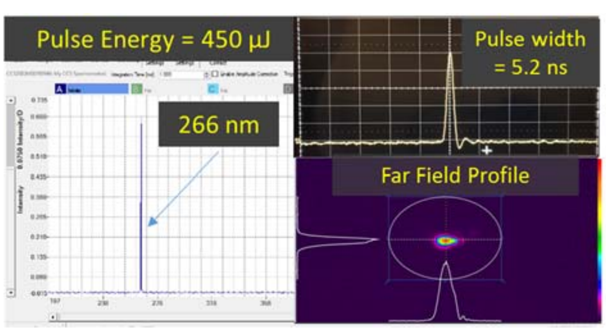

Figure 6. CORALS breadboard laser performance.

We tested the energy attenuation concept by manually rotating a half-wave plate located between the KTP and BBO crystals to rotate the 532 nm polarization relative to the BBO crystal. At a polarization rotation angle of 0° the 532 nm laser has an optimal polarization for phase matching to the BBO crystal, and therefore the conversion to 266 nm is maximized. When the polarization was rotated by 90° the conversion to 266 nm was minimized. The 266 nm laser pulse energy as a function of 532 nm polarization rotation is shown in Figure 7.

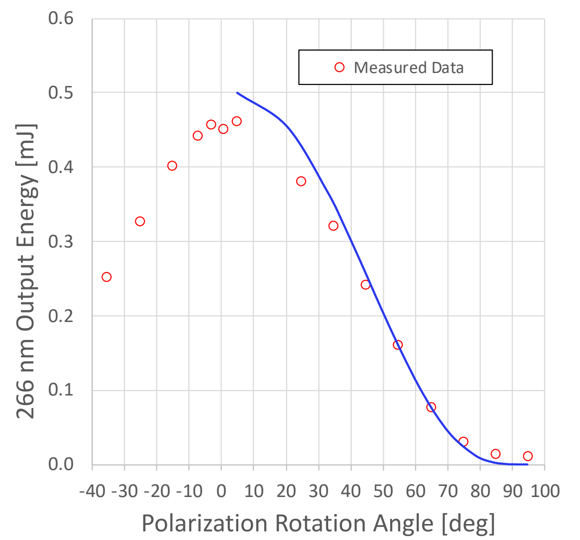

Figure 7. UV laser energy attenuation as a function of input polarization. The solid line shows the modeling results from Select Non-Linear Optics (SNLO) software [37]. The red circles represent data taken using our CORALS laser breadboard.

The CRATER laser is based on the MLA MOPA laser with emission at 1064 nm and >20 mJ with TEM_{00} mode and beam diameter of 2.2 mm. The MLA laser transmitter has been designed on the basis of the GLAS laser architecture. The laser operated nominally throughout the MESSENGER mission operations; after the spacecraft was launched in August 2004, the MLA laser accumulated more than 30 million shots. The laser transmitter was designed, built, and tested at NASA GSFC prior to delivery to the MESSENGER project. The laser was environmentally tested prior to delivery to the project for integration with the spacecraft.

The environmental tests of the laser subsystem consisted of vibration and thermal vacuum (TVAC) testing. Vibration testing consisted of three-axis random vibration to a root mean square (rms) acceleration of 8.0 *g* (where *g* is Earth's surface gravitational acceleration) in x and y, and a rms of 10.7 *g* in z, with a full evaluation of the laser pointing, power, and divergence before and after each test. The TVAC testing involved a nonoperational warm soak at 40°C, and a nonoperational cold soak at 5°C, followed by a cold start, a hot start at 35°C, and four operational thermal sweep cycles, all in vacuum conditions. During this testing the output power, divergence, beam pointing, and pointing stability were measured continually [20].

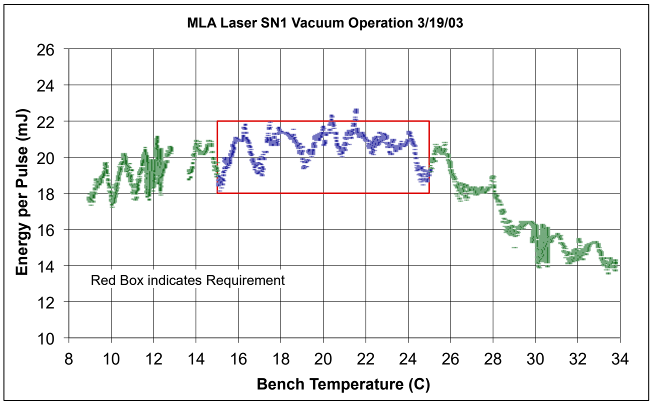

Figure 8. Output energy of the MLA laser versus bench temperature, measured in vacuum [38].

The output energy of the laser subsystem is shown in Figure 8 over a temperature sweep between 10°C and 34°C. The overall shape of the curve is due to changes in the output wavelength of the amplifier LDAs and consequent changes in absorption efficiency. The 0.8–1.5°C oscillations seen in the data are likely related to the Fabry-Perot resonances of the oscillator.

Taking advantages of the MLA design and the effort in developing the fourth harmonic wavelength for CORALS, we designed the CRATER laser with a layout as shown in Figure 4. The nonlinear frequency conversion to the fifth harmonic at 213 nm is done by mixing the fundamental at 1064 nm and fourth harmonic at 266 nm. We have modeled the conversion efficiency and optimal crystal length for the fifth harmonic generation (5HG) using a BBO crystal. Figure 9 shows the conversion efficiency of the fifth harmonic as a function of the BBO crystal length.

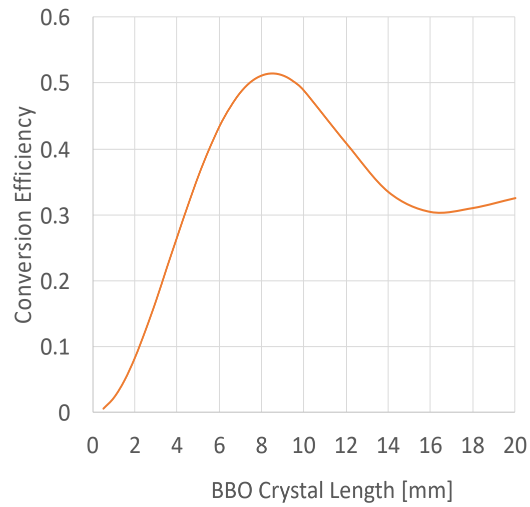

Figure 9. 213 nm conversion efficiency as function of the crystal length.

Figure 9 is based on the SNLO model with input energy of 5 mJ each for the 1064 nm and 266 nm, which is a reasonable assumption considering that 20 mJ exits the MOPA laser at 1064 nm and we send 25% of this to the BBO for 5HG (second path as described earlier) and then using 15 mJ of 1064 nm to generate 5 mJ at 266 nm, that is equivalent to a 33% conversion from fundamental to the fourth harmonic.

Using the same model, we predicted the performance of the 213 nm output with varying 1064 nm input pulse energy to mimic the use of polarization mismatch in the BBO for energy attenuation needed by the instrument. Figure 10 shows the predicted 5HG 213 nm output pulse energy and conversion efficiency as a function of 1064 nm input pulse energy, and the pulse energy attenuation as a function of input 1064 nm pulse polarization.

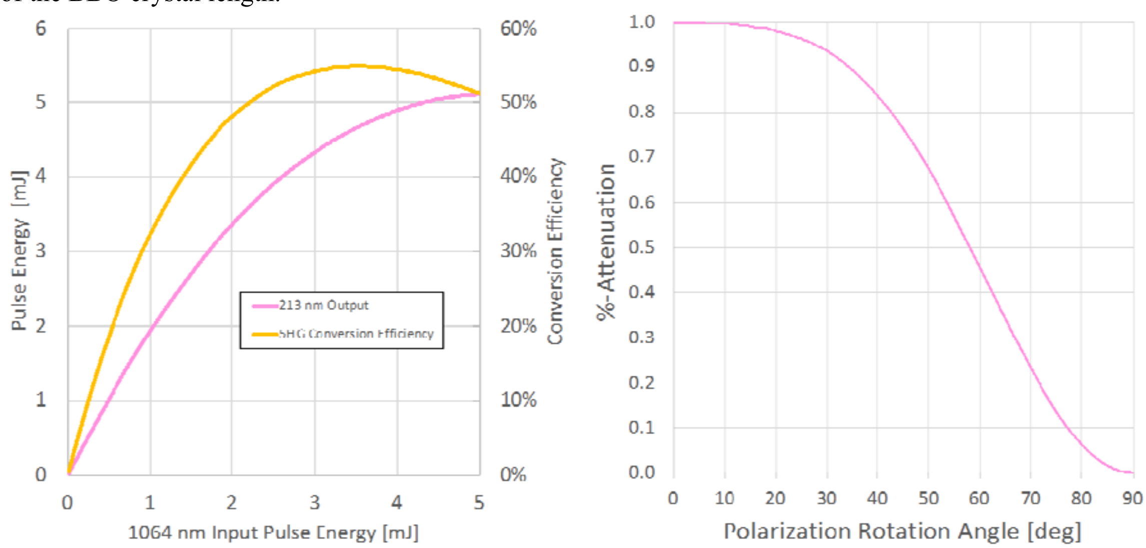

Figure 10. (left) Output pulse energy for 213 nm as a function of 1064 nm input pulse energy while maintaining a constant 266 nm input pulse energy of 5 mJ for the 5HG process. (right) Attenuation of the 213 nm output as a function of the polarization rotation angle of the 1064 nm input pulse polarization (0° is perfect phase matching).

Unlike the 4HG conversion for CORALS, 5HG requires that the input pulses for the 1064 nm and 266 nm to be reasonably synchronized in the BBO crystal. Figure 11 shows the model prediction of the 213 nm output pulse energy for the case with 0.8 mJ of 1064 nm input pulse energy and 5 mJ of 266 nm pulse energy. The maximum output pulse energy at 213 nm is predicted to be ~1.6 mJ for well synchronized input pulses. The laser will suffer a 12% reduction in output pulse energy at 213 nm if the 1064 nm and 266 nm arrival time at the BBO crystal is offset by 1 ns, which is approximately 0.4 meter in optical path length (OPL) difference. We will design our 5HG system accordingly to match the OPL between the 1064 nm and 266 nm paths to minimize unnecessary losses.

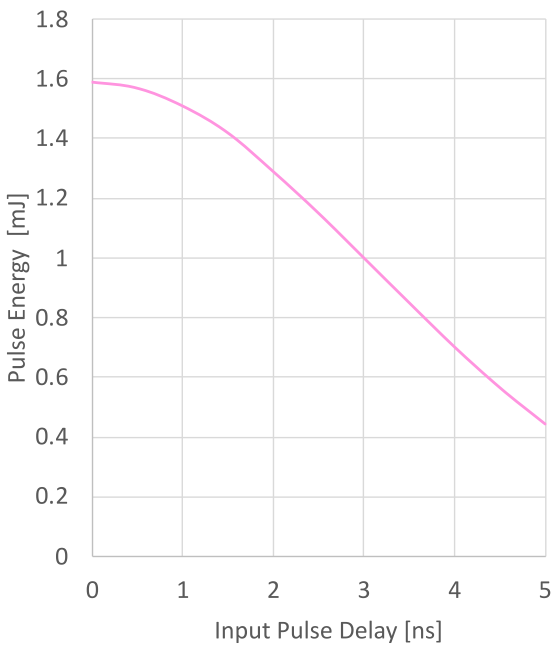

Figure 11. Output pulse energy for 213 nm beam as a function of input pulse delay between 1064 nm and 266 nm pulses.

6. Space-Flight Testing and Trade Studies

The CORALS and CRATER instruments will go through environmental testing to raise the TRL in preparation for future NASA lander mission opportunities to Europa and the Moon, respectively. The current 2-year CORALS technology development program (NASA/ICEE 2) will raise the TRL to 5 (system validation in laboratory environment). The 3-year CRATER technology development program (NASA/DALI) will raise the TRL to 6 (system demonstration in representative environment). Both lasers will go through shock and vibration testing, and DHMR bake-out at 115°C for 60 hours to reduce the risk of contaminating targeted planetary environments. Additionally, the CRATER instrument will go through a comprehensive thermal vacuum (TVAC) testing campaign.

One of the concerns for space-borne UV lasers is contamination induced laser damage [27,28,29,30,31,32,33,34,35,36]. Vacuum accelerates outgassing of organic and inorganic contaminants from polymerics and other materials used inside the laser enclosure, which may lead to adsorption or condensation on critical optical components, rendering them susceptible to laser induced damage. Our laser design minimizes (with the goal of eliminating) polymerics inside the laser enclosure. Also, the laser cavity is pressurized with CDA. Under a NASA GSFC funded internal research and development program, we are developing methodologies and techniques to use femtosecond lasers for welding dissimilar materials such as glass-to-metal, glass-to-glass, crystal-to-glass, etc. For a spaceflight laser, when opportunities arrive, we will apply this process to the UV laser build. In addition, the use of CDA will significantly lower the outgassing rate and the presence of oxygen will reduce the adsorption of contaminants (particularly organic species) on the laser optics.

Both the CORALS and CRATER lasers are based on successful flight instruments – LOLA and MLA, respectively. LOLA was launched in June 2009 and is still in operation. The lasers has accumulated over 2.5 billion shots and are still in flight operation.

The MLA instrument was launched as part of an instrument suite on MESSEGNER on August 2004 and the mission ended successfully on April 2015. This included a cruising period of seven years from Earth to insertion in the Mercury orbit. The MLA laser accumulated over 30 million shots over the life of the mission. Both lasers were designed with margin on the pump diode lifetime by derating. Proper procedures and necessary steps taken to minimize contamination induced laser damage will be key to the success of future missions.

7. Conclusion

We are developing two compact, robust, and high TRL UV lasers for the CORALS and CRATER instruments. Both lasers are based on heritage from successful previous space-flight laser instruments. Initial breadboard performance testing and analysis has been completed for the CORALS laser to validate the design and demonstrate performance. The engineering test unit (ETU) design for the CORALS laser has been peer reviewed. Computer models and analysis have been completed for the CRATER laser, and a breadboard laser build and the ETU design are in progress. The UV lasers are being developed for laser-based Orbitrap^{TM} mass spectrometer instruments for future lander mission opportunities to Europa and the Moon.

Acknowledgements

The authors acknowledge the financial support from NASA Instrument Concepts for Europa Exploration 2 (ICEE 2), and the Development and Advancement of Lunar Instrumentation (DALI) Programs.

REFERENCES

[1] Denisov, E., et al., *Orbitrap mass spectrometry with resolving powers above 1,000,000*. International Journal of Mass Spectrometry, 2012. **325-327**: p. 80-85.

[2] Olsen, J. V., et al., *Parts per Million Mass Accuracy on an Orbitrap Mass Spectrometer via Lock Mass Injection into a C-trap*. Molecular and Cellular Proteomics, 2005. **4**(12): p. 2010.

[3] Briois, C., et al., *Orbitrap mass analyser for in situ characterisation of planetary environments: Performance evaluation of a laboratory prototype*. Planetary and Space Science, 2016. **131**: p. 33-45.

[4] Bäuerle, D., *Laser Processing and Chemistry (2nd Edition)*. 1996, Berlin: Springer-Verlag. 649.

[5] Rumble Jr., J.R.E.-i.-C., ed. *Handbook of Chemistry and Physics, 100th Edition (Internet Version 2019)*. 2019, CRC Press/Taylor & Francis Group): Boca Raton, FL.

[6] Wetmore, S. D., et al., *Electron affinities and ionization potentials of nucleotide bases.* Chemical Physics Letters, 2000. **322**(1): p. 129-135.

[7] Close, D. M., *Calculated Vertical Ionization Energies of the Common α-Amino Acids in the Gas Phase and in Solution.* The Journal of Physical Chemistry A, 2011. **115**(13): p. 2900-2912.

[8] Holm, A. I. S., et al., *Dissociation and multiple ionization energies for five polycyclic aromatic hydrocarbon molecules*. The Journal of Chemical Physics, 2011. **134**(4): p. 044301.

[9] Russo, R. E., et al., *Influence of wavelength on fractionation in laser ablation ICP-MS.* Journal of Analytical Atomic Spectrometry, 2000. **15**(9): p. 1115-1120.

[10] Zenobi, R. and Knochenmuss, R., *Ion formation in MALDI mass spectrometry*. Mass Spectrometry Reviews, 1998. **17**(5): p. 337-366.

[11] Managadze, G. G., et al., *Study of the main geochemical characteristics of Phobos' regolith using laser time-of-flight mass spectrometry.* Solar System Research, 2010. **44**(5): p. 376-384.

[12] Goetz, W., et al., *MOMA: The challenge to search for organics and biosignatures on Mars*. International Journal of Astrobiology, 2016. **15**(3): p. 239-250.

[13] Arevalo Jr., R., et al., *Design and Demonstration of the Mars Organic Molecule Analyzer (MOMA) on the ExoMars 2018 Rover.* IEEE Aerospace Conference, 2015. p. 1-11.

[14] Goesmann, F., et al., *The Mars Organic Molecule Analyzer (MOMA) Instrument: Characterization of Organic Material in Martian Sediments.* Astrobiology, 2017. **17**(6-7): p. 655-685.

[15] Li, X., et al., *Mars Organic Molecule Analyzer (MOMA) laser desorption/ionization source design and performance characterization.* International Journal of Mass Spectrometry, 2017. **422**: p. 177-187.

[16] Büttner, A., et al., *Optical design and characterization of the MOMA laser head flight model for the ExoMars 2020 mission*. Proc. SPIE 11180, International Conference on Space Optics, 2019.

[17] Weßels, P., et al., *UV-DPSS laser flight model for the MOMA instrument of the ExoMars 2020 Mission.* Proc. SPIE 11180, International Conference on Space Optics, 2019.

[18] Arevalo Jr, R., et al., *An Orbitrap-based laser desorption/ablation mass spectrometer designed for spaceflight.* Rapid Communications in Mass Spectrometry, 2018. **32**(21): p. 1875-1886.

[19] Yu, A., et al., *The Lunar Orbiter Laser Altimeter (LOLA) laser transmitter.* Proceedings 2011 IEEE International Geoscience and Remote Sensing Symposium, 2011. p. 3378-3379.

[20] Krebs, D. J., et al., *Compact passively Q-switched Nd:YAG laser for the MESSENGER mission to Mercury.* Applied Optics, 2005. **44**(9): p. 1340-1343.

[21] Afzal, R. S., et al., *The Geoscience Laser Altimeter System (GLAS) Laser Transmitter.* IEEE Journal of Selected Topics in Quantum Electronics, 2007. **13**(3): p.511-536.

[22] Ciapponi, A., et al., *Non-linear optical frequency conversion crystals for space applications.* Proceedings of SPIE LASER, 2011. **7912**: p. 13.

[23] Konoplev, O. A., et al., *Three-year aging of prototype flight laser at 10 kHz and 1 ns pulses with external frequency doubler for ICESat-2 mission.* Proceedings Laser Technology for Defense and Security XII, 2016. **9834**.

[24] Smith, A. V., et al., *Increased acceptance bandwidths in optical frequency conversion by use of multiple walk-off-compensating nonlinear crystals*, J. Opt. Soc. Am. B, 1998. **15**(1): p. 122.

[25] Wang, H., and Weiner, A.M., *Efficiency of short-pulse type-I second-harmonic generation with simultaneous spatial walk-off, temporal walk-off, and pump depletion*. IEEE Journ. Quantum Electronics, 2003. **39**(12): p. 1600.

[26] Droz, C., et al., *Walk-off Compensated 266-nm Generation with Two β-BaB2O4 Crystals*. Optical

Review, 1999. **6**(2): p. 97.

[27] Kokkinos, D., et al., *Laser optics in space failure risk due to laser induced contamination*. CEAS Space J, 2017. **9**(2): p. 153-162.

[28] El Reaidy, G. G., et al., *Study of the first stages of laser-induced contamination.* Optical Engineering, 2018. **57**(12): 121903.

[29] Schröder, H., et al., *Investigation of laser induced deposit formation under space conditions.* Proc. SPIE, 2018. 10566, 105661K, 2018.

[30] Wernham, D., *Optical coatings in space*. Proc. SPIE 8168, 81680F, 2011.

[31] Schroeder, H., et al., *Laser-induced contamination and its impact on laser damage threshold*. Proc. SPIE 8885, 88850R, 2013.

[32] Riede, W., et al., *Laser-induced contamination on space optics*. Proc. SPIE 8190(1), 81901E, 2011.

[33] Ließmann, M., et al., *Scaling of laser-induced contamination growth at 266nm and 355nm*," Proc. SPIE 9632, 96321Z. 2015.

[34] Tighe, A. P., et al., *Growth mechanisms for laser induced contamination on space optics in vacuum.* Proc. SPIE 7132, 71321L, 2008.

[35] Wernham, D., et al., *Laser-induced contamination mitigation on the ALADIN laser for ADM-aeolus*. Proc. SPIE 7842, 78421E, 2010.

[36] Alves, J., et al., *Laser-induced contamination control for high-power lasers in space-based lidar missions*. Proc. SPIE 10565, 1056524, 2010.

[37] SNLO nonlinear optics code available from A. V. Smith, AS-Photonics, Albuquerque, NM

[38] Yu, A. W., et al., *In-flight performance of the Mercury Laser Altimeter laser transmitter*. Proc. SPIE Solid State Lasers XXIII: Technology and Devices, 2014. **8959**.

BIOGRAPHY

Molly Fahey *is a laser scientist in the Laser and Electro-Optics Branch at Goddard Space Flight Center where she supports the development of laser hardware and electro-optic components for current and future Earth science, Planetary science, Heliophysics, and Astrophysics space flight programs. She received a BA in Physics from the College of St. Benedict/St. John's University, St. Joseph, MN in 2005, and a MS in Mechanical Engineering from Florida Institute of Technology, Melbourne, FL in 2007.*

Anthony Yu *is a laser scientist and branch technologist in the Lasers and Electro-Optics Branch at NASA Goddard Space Flight Center. He has over 30 years of experience in space-based laser development for Earth and planetary science applications. He earned a BS in Physics from the University of Central Florida in 1982, an MS and PhD in Physics from Georgia Institute of Technology in 1984 and 1988. He is a senior member of the IEEE and Optical Society of America.*

Andrej Grubisic *is a research scientist in the Planetary Environments Laboratory at NASA Goddard Space Flight Center. He received his Ph.D. in Chemistry from the Johns Hopkins University and was an NRC/NIST postdoctoral fellow at JILA – University of Colorado. With extensive experience in ultrafast laser technology, mass spectrometry, as well as electron and optical microspectroscopy, he is broadly interested in the development of, both, space-flight and field-portable instrumentation for sensitive chemical detection and identification. His current research focuses on the advancement of miniature high-performance mass spectrometers and implementation of novel ionization schemes that hold potential to minimize sample handling on future planetary missions.*

Dr. Stephanie Getty *is a planetary research scientist and the Deputy Director of the Solar System Exploration Division at NASA Goddard Space Flight Center. Her research interests are in the area of science instrument development for in situ planetary missions, particularly in the pursuit of understanding the origin, evolution, and processing of organic chemistry in our Solar System. She is a member* *of the ExoMars Rover Mars Organic Molecule Analyzer science team.*

Ricardo Arevalo Jr. *is an Associate Professor of Geology at the University of Maryland, College Park, the same department he received his Ph.D. from in 2010. He serves as Principal Investigator for the CORALS and CRATER investigations, and a Science Team Member for the Mars Organic Molecule Analyzer (MOMA) instrument onboard the ExoMars rover. His research interests are centered on the chemical analysis and geochemical modeling of planetary systems, in situ laser desorption/ablation microprocessing and mass spectrometry, and developing next generation instrumentation for planetary missions.*

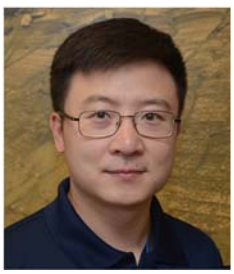

Xiang Li *received his B.S. in Chemistry from the Peking University, China in 2003, and Ph.D. in Physical Chemistry from the Johns Hopkins University in 2009. He is an assistant research scientist with a joint appointment at the University of Maryland, Baltimore County and NASA Goddard Space Flight Center. His research focuses on the detection of trace element and astrobiologically relevant organic molecules in planetary systems, like Mars. He is especially interested in the instrument development of time-of-flight and ion trap mass spectrometers with various ionization and ion gating techniques. He serves as a mass spec. scientist for the MOMA ion trap MS on ExoMars, and Co-I on development of LITMS and MACROS instrument.*

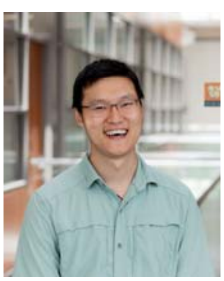

Richard (Dicky) Liu *is a graduate student from the University of Illinois at Urbana-Champaign, where he is pursuing a PhD in Electrical Engineering. His research with Prof. Can Bayram investigates the growth of polarization-free cubic phase III-nitride-based photonic devices on silicon substrates. These semiconductors have the potential to increase efficiency and brightness, reduce cost, and cover the full visible light spectrum for the next gen solid-state lighting and displays. Dicky has published four first-author journal papers and holds a patent. He is a NASA Space Technology Research Fellow (NSTRF, NSTGRO), and had worked at NASA Goddard Space Flight Center.*

William Mamakos *founded Design Interface Inc. in 2001. Design Interface is an established company that is focused on providing professional Design Engineering Services serving Government and Commercial markets, as well as the research and science communities. Mr. Mamakos has designed and developed complex mechanical, optical-mechanical, electro-mechanical instruments and mechanisms for ground based, airborne and spaceborne instruments and payloads for over 37 years. Specializing in precision spaceborne optical instruments, lasers and mechanisms as well as electronic packaging of high voltage electronics, power converters and detectors.*